Fiber Spinning from Poly(propylene)–Organoclay Nanocomposite

Silvia Pavliková,[1] Ralf Thomann,[2] Peter Reichert,[2] Rolf Mülhaupt,[2] Anton Marcinčin,[1] Eberhard Borsig,[1,3]

[1]*Department of Fiber and Textile Chemistry, Faculty of Chemical and Food Technology, Slovak University of Technology, Radlinského 9, 812 37 Bratislava, Slovak Republic*
[2]*Freiburger Materialforschungszentrum und Institut für Makromolekulare Chemie der Albert-Ludwigs Universität, Stefan Meier Str. 31, D-79104 Freiburg, Germany*
[3]*Polymer Institute, Slovak Academy of Sciences, Dúbravská cesta 9, 842 36 Bratislava, Slovak Republic*

Received 11 April 2002; accepted 29 July 2002

ABSTRACT: SOMASIF ME C16, a filler that enables generation of anisotropic nanoparticles by *in situ* exfoliation of organic layered silicates, was melt compounded with poly(propylene) (PP) in the presence of maleic anhydride-grafted PP. Fibers were prepared from this composite by a spinning procedure. The prepared anisotropic fibers were partially oriented by using different drawing ratios. The morphological study showed that the drawing ratio of the fibers particularly influences the level of exfoliation of the SOMASIF ME C16 where the nanoparticles are formed. The layered sheets of the SOMASIF particles are oriented in the direction of the fiber axis. The tensile strength of the filled fibers increases with the increase of drawing ratio much more than that of unfilled PP fibers. This result is accounted for by the formation of exfoliated structures from the nanoparticles of SOMASIF ME C16 by fiber drawing. © 2003 Wiley Periodicals, Inc. J Appl Polym Sci 89: 604–611, 2003

Key words: poly(propylene); nanocomposites; fibers; morphology

INTRODUCTION

Polymer nanocomposites based on the incorporation of inorganic or organic filler have attracted considerable attention not only from researchers but also from producers of polymer materials.[1–13] The reason for the interest is that such modification generally promises an improvement in the mechanical and utility properties of the polymer, in particular increased toughness or decreased flammability.[2] This method of polymer property improvement was used in this study of isotactic poly(propylene) (PP), which belongs to the most environmentally friendly and versatile of the commercial plastics. The increase of dimensional stability, heat distortion temperature, stiffness, strength, and impact resistance without sacrifice of ease of processability can increase the competitiveness of a PP for use in resins applications.[2] For this purposes, the same nanofiller as in our previous work[2] (i.e.. the synthetic fluorine-containing hectorite SOMASIF ME C16) was used. This nanofiller is obtained by heating talcum with Na_2SiF_6, which is then rendered organophilic by ion exchange of sodium cations located in the interlayer galleries with primary hexadecylamine. This kind of filler (SOMASIF ME C16) enables one to generate anisotropic nanoparticles by *in situ* exfoliation of organic layered silicates.[7] Previous work has shown that a nanocomposite was obtained when SOMASIF ME 100 was melt compounded with PP in the presence of maleic anhydide-grafted PP (PP-g-MA).[2]

This study is a continuation of our previous basic study[2] of a series of PP nanocomposites, in which both the effect of one-dimensional orientation of the nanocomposite in the form of fibers and the influence of PP-g-MA compatibilizer on the mechanical properties of the nanocomposite fibers was investigated.

EXPERIMENTAL

Materials

Organophilic layered silicates were prepared from SOMASIF ME (100) (CO-OP Chemical Company, Japan) and hexadecylamine in a procedure described elsewhere.[2]

Preparation of poly(propylene) nanocomposites

Poly(propylene) (PP) powder and the organoclay were premixed in a tumbling mixer with 0.25 wt % stabilizer (Irganox 1010/Irgafos 168 Ciba 4/1). This mixture was melt blended with 10 wt % PP-g-MA [Hostaprime H C5, Clariant GmbH; maleic anhydride (MA) content of 4.2 wt %; M_w = 32.000 g/mol; T_m = 152°C] in a co-rotating twin-screw extruder (Werner

Correspondence to: E. Borsig (borsig@chelin.chtf.stuba.sk).

Journal of Applied Polymer Science, Vol. 89, 604–611 (2003)

& Pfleiderer; ZSK 25) at 190–230°C and at 300 rpm. In this way, PP nanocomposite samples containing 1, 2, and 5 wt % of organoclay were prepared.

Spinning of the nanocomposites

The composite fibers containing 1, 3, and 5 wt % of SOMASIF were prepared from granulated polymer with a laboratory TS φ 16-mm extruder using a spinning nozzle with 13 spinnerets of 0.05-mm diameter each under the following conditions: homogenization zone, 250°C; and spinning speed, 150 m min^{-1}. In this way, partially oriented isotropic fibers were prepared and drawn with different draw ratios ($\lambda = 2$ or 3).

Tensile strength measurement

The mechanical properties of the composite fibers were determined with an INSTRON 1112 apparatus at ambient temperature. Clamping length and deformation rate were 100 mm and 500 mm min^{-1}, respectively. Ten specimens of each composition were tested and the average values are reported.

Rheological measurements

The rheological properties (shear speed and viscosity) of the fiber-forming polymers were measured on a Plastometer VP-05 at 250°C and at five values of shear stress τ. Melt flow index was recorded as the amount (grams) of molten polymer passing through a fixed capillary under constant pressure at 250°C in 10 min.

Atomic force microscopy (AFM)

Atomic force microscopy (AFM experiments were performed with a Nanoscope III scanning probe microscope. Height and phase images were obtained simultaneously while operating the instrument in the tapping mode under ambient conditions. Images were taken at the fundamental resonance frequency of the Si cantilevers, which was typically around 300 kHz. Typical scan speeds during recording were 0.3–1 line/s, using scan heads with a maximum range of 16 $\times$ 16 μm. The phase images represent the variations of relative phase shifts (i.e., the phase angle of the interacting cantilever relative to the phase angle of the freely oscillating cantilever at the resonance frequency) and are thus able to distinguish materials (e.g., amorphous and crystalline polymers) by their material properties.

Transmission electron microscopy (TEM)

TEM measurements were carried out with a LEO OMEGA 912 transmission electron microscope applying an acceleration voltage of 120 keV. The specimens were prepared by embedding the fibers in "LR white" embedding media and sectioned with an ultramicrotome equipped with a cryochamber.[12]

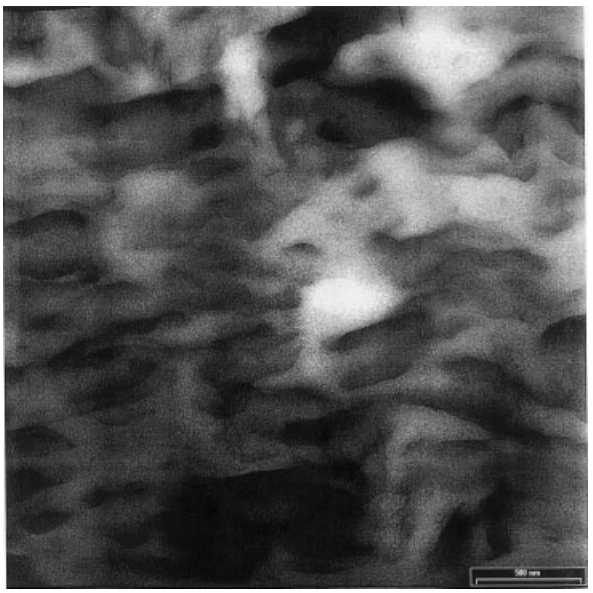

Figure 1 TEM micrograph of PP nanocomposite fiber containing 1% nanoparticles of SOMASIF MEC 16 (parallel cut of E23; $\lambda = 3$).

RESULTS AND DISCUSSION

Morphology of the nanocomposite PP fibers

TEM micrographs were prepared from PP fibers with drawing ratios (λ) of 3 and 2, containing various quantities of the filler SOMASIF ME C16.[2] In the case of the PP composite fiber containing 1% SOMASIF filler, prepared at $\lambda = 3$ and cut parallel to the fiber (Figure 1, Sample E 23-3-500/P), almost the entire area of the section is filled with small, planar particles of oblong shape. These particles have a typical length of $\geq$750 nm and a width of $\sim$200 nm. All these particles are oriented in the drawing direction of the fiber (i.e., from left to right in this case). The transparent appearance of the particles indicates that they are built up by a small number of SOMASIF layers. Some of the particles seem to be clearer (transparent) than others. The leaf-like sheets are considered to be single exfoliated layers of SOMASIF.

A vertical cut of the fiber is shown in Figure 2 (Sample E23-3-2000). The visible length of the particles corresponds to the width of the particles shown in Figure 1, indicating that the plate-shaped particles of SOMASIF are oriented in the direction of fiber drawing (i.e., perpendicular to the plane of the image). Therefore, the length of the particles ($\sim$750 nm; see Figure 1) is not visible.

A higher magnification of the same sample is shown in Figure 3 (Sample E 23-3-2000). The more detailed

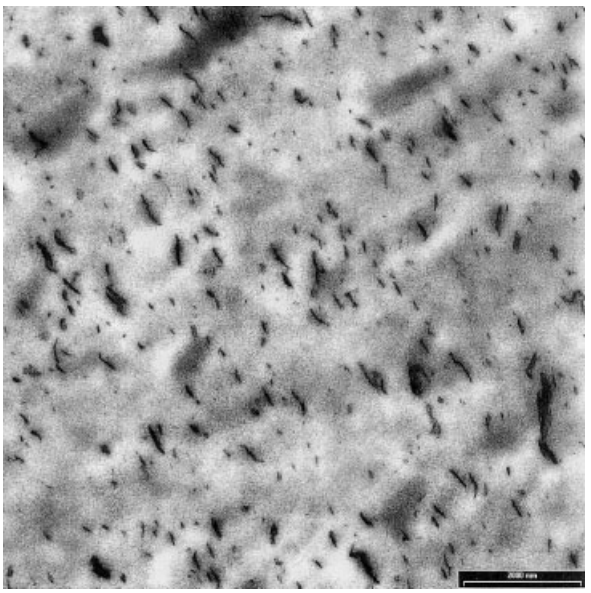

Figure 2 TEM micrograph of PP nanocomposite fiber containing 1% nanoparticles of SOMASIF MEC 16 (vertical cut of E23; $\lambda = 3$).

micrograph confirms a high degree of exfoliation. Typically, two or three layers of SOMASIF form the particles, but single layers and larger stacks of layers are also visible. Again, only the particles of ~200 nm width are visible. In some regions, particles with a flat-on orientation are visible. This orientation indicates that during the spinning and drawing, not all particles of the filler managed to orient themselves in such a way that they are all completely parallel to the axis of the fiber (in this case, we would see the edge-on shape of the particles only). The distance between adjacent layers of the filler is ~10 nm. The exfoliation of the SOMASIF appears during both the preparation of the PP–SOMASIF composite in an extruder and also during the spinning and drawing process. The layered sheets of SOMASIF particles are oriented in the direction of the fiber axis (i.e., in the direction of fiber drawing). In this direction, exfoliation of the SOMASIF filler also occurs. This orientation and exfoliation are most probably the reasons that almost the whole area of the micrograph of the parallel-cut fiber is filled in with SOMASIF sheets, as indicated in Figure 1 (Sample E23-3-500/P).

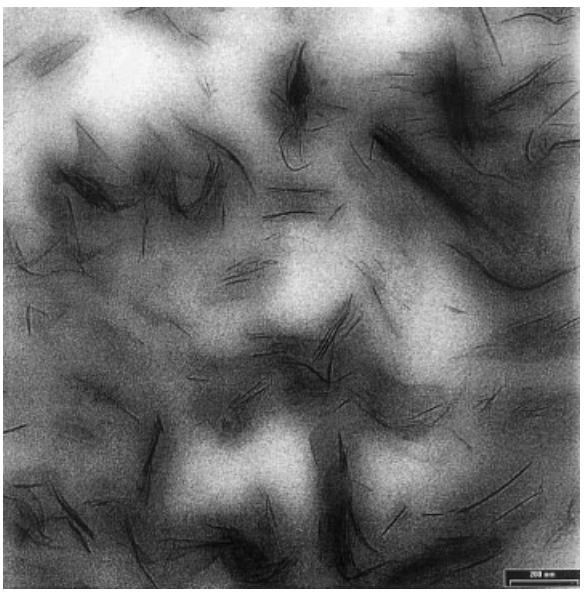

Figure 3 TEM micrograph of PP nanocomposite fiber containing 1% nanoparticles of SOMASIF ME C16 at a higher magnification (vertical cut of E23; $\lambda = 3$).

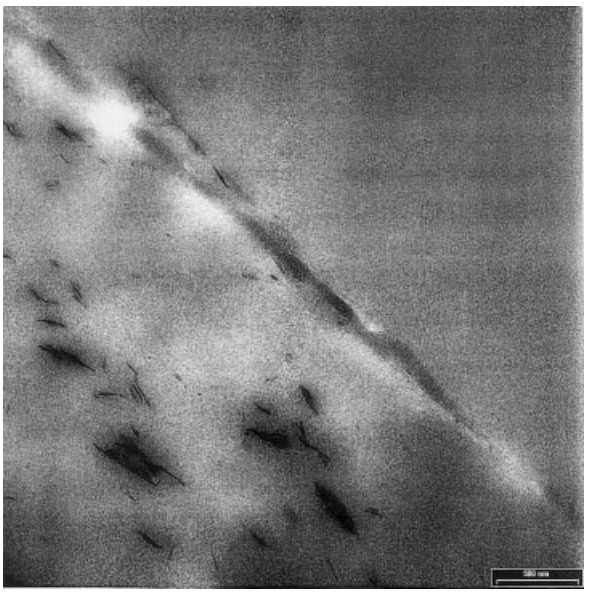

Figure 4 TEM micrograph of PP nanocomposite fiber containing 1% nanoparticles of SOMASIF MEC 16 (vertical cut of E23, $\lambda = 3$).

An interesting region is the surface of the vertically cut fiber. (Figure 4, Sample E 23-3-500R/S). This part of the fiber is termed by the specialist as a "fiber skin". The particles of the filler that are situated in the "fiber skin" or in its vicinity are oriented parallel to the edge of the fiber, and in some cases it seems that the SOMASIF layers were excluded from the PP fiber.

In the case of PP fiber filled with 5% SOMASIF and $\lambda = 2$ (Figure 5, Sample E22-1000/S), the micrograph of the vertically cut fibers provides, as expected, an indication of a higher density of the dispersed SOMASIF particles. Also, the particles are oriented in the direction of drawing. As seen in Figure 6 (E22-200/S), exfoliation of the SOMASIF particles also takes place but is less pronounced than in the case of fiber filled with 1% SOMASIF and with higher drawing ratio (i.e., $\lambda = 3$). A higher density is also supported by the observed greater thickness of the small plate-like particles of the same filler, SOMASIF, in the fiber (Figure 6, Sample E22-200/S).

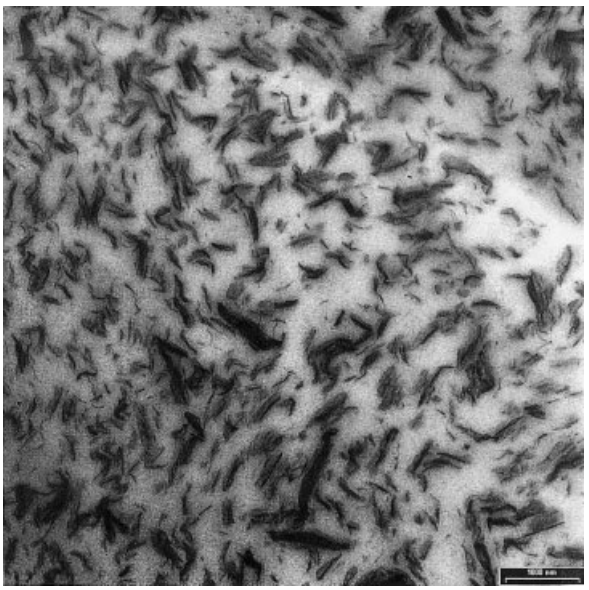

Figure 5 TEM micrograph of PP nanocomposite fiber containing 5% nanoparticles of SOMASIF ME C16 (vertical cut of E22; $\lambda = 2$).

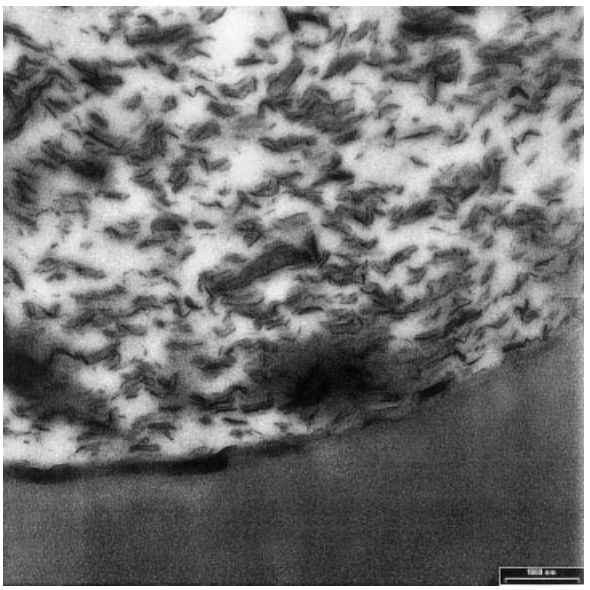

Figure 7 TEM micrograph of PP nanocomposite fiber containing 5% nanoparticles of SOMASIF ME C16 (the edge of E22; $\lambda = 2$).

The micrograph in Figure 7 shows the edge of the fiber. Again, the enrichment of the surface with SOMASIF particles is clearly visible. The micrograph of the fiber skin depicted at higher magnification (Figure 8) shows some SOMASIF particles located directly at the surface of the fiber. In this image, the PP matrix appears bright and the surrounding embedding media darker. It is interesting to see that the particles on the surface are either not covered or only partially covered by PP.

Exfoliated particles with relatively large oblong planes (similar to Figure 1, Sample E23-3-500/P) are seen in the micrographs of parallel-cut PP fiber filled with SOMASIF and $\lambda = 2$ (Samples E22-2-200/p/a and E 22-200/P in Figures 9 and 10, respectively). These particles have a length >1 μm. As already mentioned, it is clearly visible that the particles are thicker and less exfoliated than in the previous case (Figure 3, E 23-3-500/P). Partly exfoliated particles in a side section, like a cluster of foils, are also evident in Figure 10 (E 22-200/P). The level of orientation of the parti-

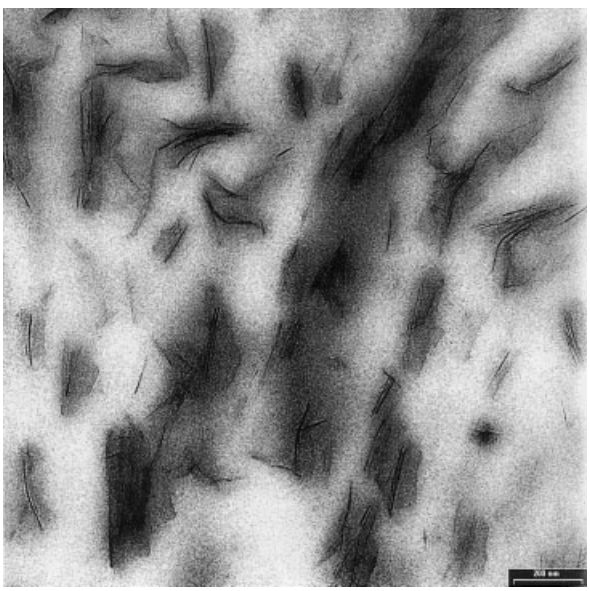

Figure 6 TEM micrograph of PP nanocomposite fiber containing 5% nanoparticles of SOMASIF ME C16 (vertical cut of E22; $\lambda = 2$).

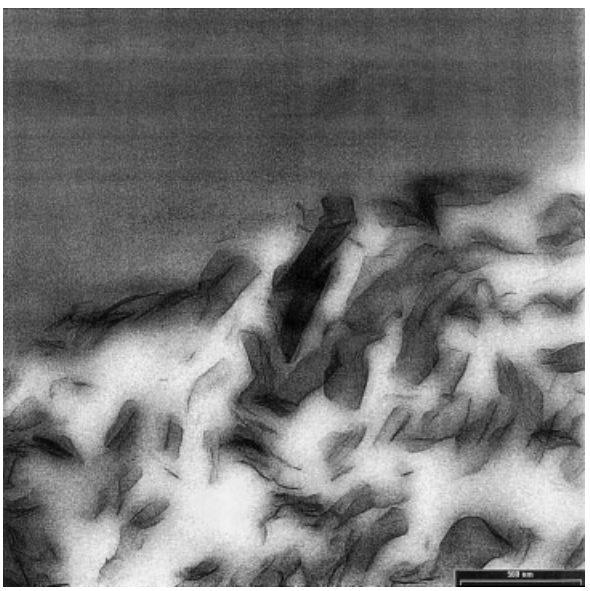

Figure 8 TEM micrograph of PP nanocomposite fiber containing 5% nanoparticles of SOMASIF ME C16 (the edge of E22; $\lambda = 2$).

Figure 9 TEM micrograph of PP nanocomposite fiber containing 5% nanoparticles of SOMASIF ME C16 (parallel cut of E22; $\lambda = 2$).

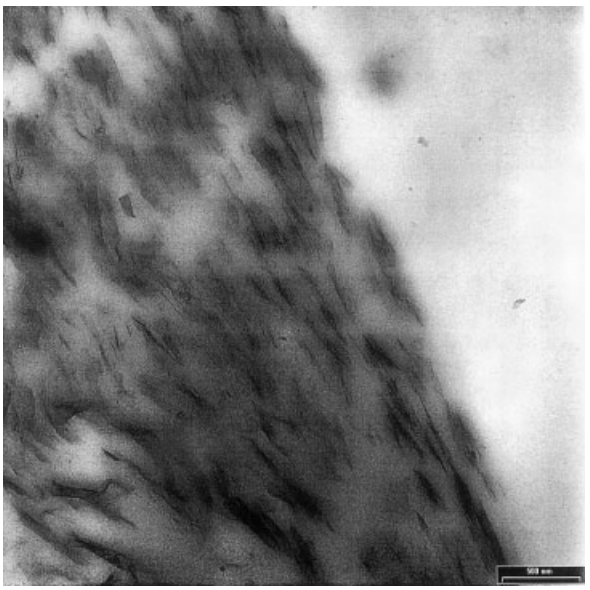

Figure 11 TEM micrograph of PP nanocomposite fiber containing 5% nanoparticles of SOMASIF ME C16 (parallel cut of E22; $\lambda = 2$).

cles in the direction of fiber drawing is slightly lower, which corresponds well to the perpendicular cut sections shown in Figures 5–8.

The skin of the fiber is visible in the parallel cut of the PP shown in Figure 11 (E 22-500/P-S). The particles of the filler are very close to the surface of the fibers and, in some cases, it seems that they form a part of the fiber surface.

The micrographs of the vertical cut of PP fiber filled with 5% SOMASIF and $\lambda = 2$ show that drawing ratio has a considerable influence on the extent of exfoliation of the SOMASIF and also on orientation of the exfoliated particles in the PP fiber.

The morphology of the surface of the fibers is shown in the AFM micrographs in Figures 12–14. Figure 12 shows the tapping mode/phase mode image of the surface of unfilled PP fiber. The tapping mode/phase mode shows the material properties of the sample. Crystalline material appears bright and amorphous material appears darker. The unfilled fiber shows typical fibrils of PP orientated in the drawing direction of the fiber A

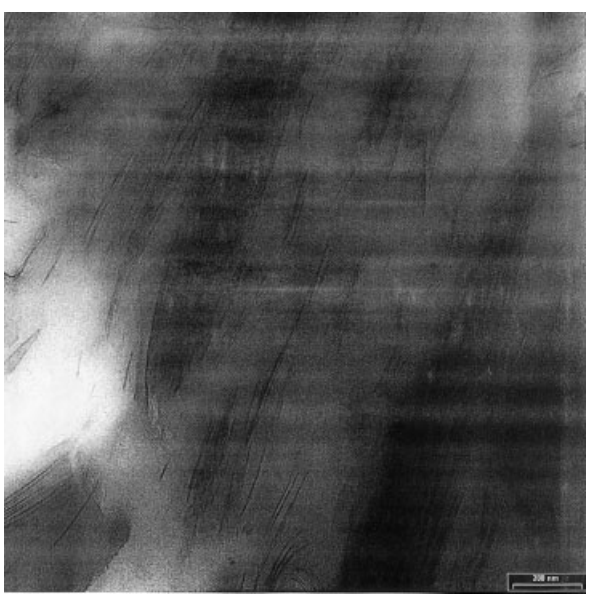

Figure 10 TEM micrograph of PP nanocomposite fiber containing 5% nanoparticles of SOMASIF ME C16 (parallel cut of E22; $\lambda = 2$).

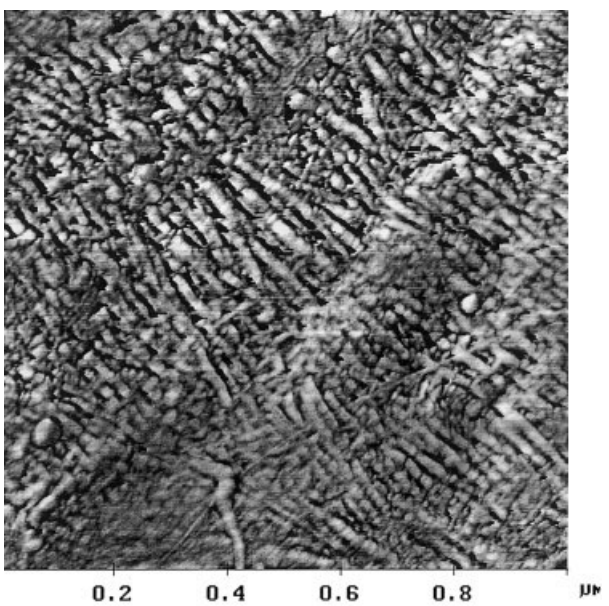

Figure 12 AFM micrograph fiber surface of the E22 containing 5% nanoparticles of SOMASIF ME C16 ($\lambda = 2$).

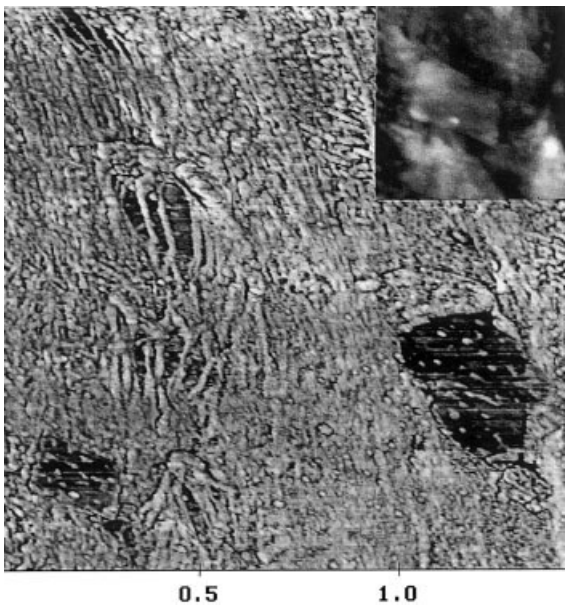

Figure 13 AFM micrograph fiber surface of the E22 containing 5% nanoparticles of SOMASIF ME C16 ($\lambda = 2$).

close look on the fibrils shows perpendicular-orientated stacks of lamellae within the fibers. These lamellae are the results of a recrystallization of the PP after the breakup of the original lamellae during the drawing process. In contrast to the unfilled fiber, the filled fiber (Figure 13) confirms the appearance of SOMASIF particles on the surface (dark). The surface seems to be quite "bumpy", and some parts of the filler particles occur on the surface without being covered by a closed PP layer. In some cases, these particles are crossed by PP fibrils (e.g., the two particles in the upper left corner of the image). The inset of Figure 13 shows the height mode image of the SOMASIF particle visible in the lower left corner, which indicates that the plate-like shaped SOMASIF particle is clearly separated from the PP fiber in this case. The observed exclusion of SOMASIF particles from the fiber is in agreement with the TEM results shown in Figures 7 and 8. The height profiles taken on the surface of the filled and unfilled fiber in the drawing direction are shown in Figure 14. The surface roughness of the unfilled fiber (bottom) is caused by the PP fibrillation and the crystallinities. The filled fiber (top) appears rougher. The observed correlation between the surface roughness and the filler content is not only the result of excluded SOMASIF particles because it also exists in areas without visible SOMASIF particles. This result suggests that particles within the fiber also have an influence on the surface roughness.

Mechanical properties of the PP nanocomposite fibers

Tensile strength measurements

The PP nanocomposite was prepared by compounding PP in the presence of the synthetic fluorine-containing hectorite filler SOMASIF ME100. This filler was obtained by heating talcum with Na_2SiF_6, abbreviated as ME, and then rendering ME organophilic by ion exchange with alkyl amines of different alkyl chain lengths. In addition to PP and filler, also included in the composite mixture was the compatibilizer PP-g-MA containing 4.2 wt % MA groups. This additive was studied in our previous study of mechanical properties[2] where it was found that both PP-g-MA compatibilizer and alkyl chain length of the amine group in the modified filler had a dramatic impact on Young's modulus and yield stress of the nanocomposites.

The filler SOMASIF C16, consisting of layered silicate modified with hexadecyl amine, was selected for this study. Three PP nanocomposite samples were prepared with 1, 3, and 5 wt % of the modified silicate and with 10 wt % PP-g-MA compatibilizer containing 4.2 wt % MA. All samples of the nanocomposite were subjected to a spinning procedure using laboratory spinning equipment (extruder diameter, $\varphi = 16$ mm) at 250°C. The extruded nanocomposite fibers were drawn on a vertical elongation device and then submitted for tensile strength and ductility measurements with an Instron Type 1112 apparatus. The fiber sample containing 1 wt % nanocomposite (Sample E23) with $\lambda = 2$ showed considerable decrease of tensile strength from 2.81 to 0.65 cN/dtex in comparison with unfilled PP fibers. This decrease in tensile strength is caused by the presence of 10% PP-g-MA compatibilizer. PP

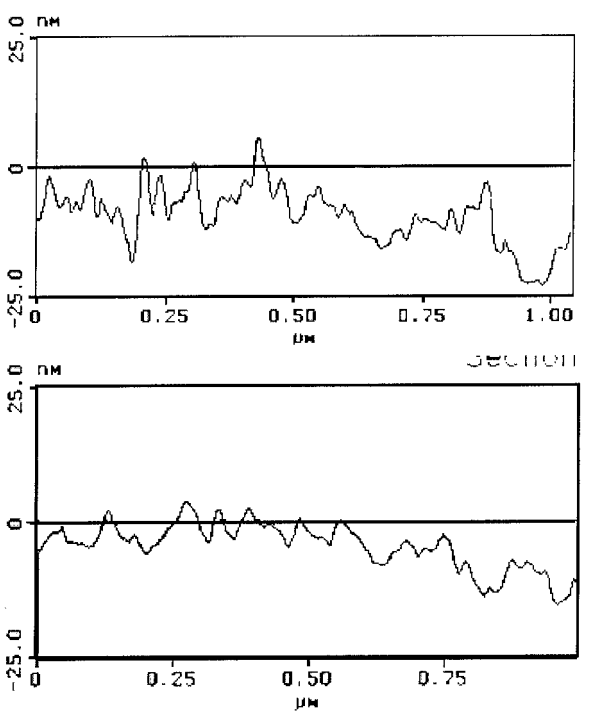

Figure 14 Height profiles taken by AFM on the surface of (a) the filled and (b) unfilled fiber (containing 5% nanoparticles of SOMASIF ME C16) in the drawing direction ($\lambda = 2$).

TABLE I
Tensile Strength of the Nanocomposite PP Fibers Filled with SOMASIF MEC16

Parameter	PP (alone)		PP + SOMASIF MEC 16					
			Sample E23 SOMASIF 1 wt %		Sample E23/22 SOMASIF 3 wt %		Sample E22 SOMASIF 5 wt %	
Melt flow index [g/10 min]	4.26		7.97		8.14		9.06	
Drawing ratio	$\lambda = 2$	$\lambda = 3$	$\lambda = 2$	$\lambda = 3$	$\lambda = 2$	$\lambda = 3$	$\lambda = 2$	$\lambda = 3$
Fineness [dtex]	328.40	220.40	361.47	257.65	363.92	253.76	360.13	252.13
Tensile strength [cN/dtex]	2.81	3.09	0.65	1.46	0.83	1.66	1.34	2.30
Elongation [%]	33.35	28.50	32.30	26.15	32.15	26.12	32.35	25.70

grafted with MA usually has a much lower molecular weight than the original polymer because of the simultaneous degradation of PP during the grafting reaction. Similar diminished tensile strengths have been observed with PP fibers containing PP-g-MA alone (without filler). In general, the compatibilizer has considerable influence on the tensile strength of the fibers.[14] Nevertheless, an increase in the nanocomposite filler in the PP fibers to 3 and 5 wt % (Sample E23/22 and Sample E22, respectively), with preparation at the same drawing ratio of $\lambda = 2$, resulted in increases in tensile strengths to 0.83 and 1.34 cN/dtex, respectively (Table I). This observation is in accord with the previous measurements of non-oriented PP nanocomposite samples.[2]

The most pronounced effect seems to be the influence of the level of orientation (elongation) of the nanocomposite PP fibers. In the case of nanocomposite fibers with 1 wt % filler (Sample E23), the increase in drawing ratio from $\lambda = 2$ to $\lambda = 3$ resulted in a dramatically increased tensile strength from 0.65 to 1.46 cN/dtex (Table I). Also, with fibers containing 3 and 5 wt % filler (Sample E23/22 and Sample E22, respectively), tensile strength increased practically twofold when the drawing ratio increased from $\lambda = 2$ to $\lambda = 3$.

We assume that two effects, which were also observed in the morphological study of the PP composite fibers, should contribute to the increase of the reinforcement efficiency of the filler in the fibers: (1) the very efficient exfoliation of the SOMASIF filler particles in the PP composite fibers brought about by drawing after spinning. And (2) the considerable increase of the content of self-assembled exfoliated structures in the fibers.

The previous AFM study of the exfoliation of the same type of filler showed that the melt processing promoted breakup of the original silicate filler particles and that nanoparticles were generated by *in situ* exfoliation of organophilic layered silicates. Therefore, it was expected that the elongation of nanocomposite PP fibers would contribute to an increase in the level of exfoliation of the filler particles, which has been shown in this morphological study. The influence of the drawing ratio of the fibers on the level of exfoliation of filler particles is shown in Figure 3, which is a micrograph of a vertical cut of nanocomposite fiber with a drawing ratio of $\lambda = 3$, and in Figure 6, which is a micrograph of a sample with a drawing ratio of $\lambda = 2$. The average number of layers of filler particles is much higher with $\lambda = 2$ than with $\lambda = 3$ (Figure 3). This result indicates that there is a direct proportionality between drawing ratio (elongation) of the fibers and the level of exfoliation. In addition to higher tensile strength, fibers obtained at the higher drawing ratio (i.e., $\lambda = 3$) had a greater amount of self-assembled exfoliated structures on a higher level than fibers prepared at drawing ratio of $\lambda = 2$ (with the same original content of SOMASIF filler of 1 wt %; Sample E23). So, it can be concluded that the higher level of self-assembled exfoliated structures in PP nanocomposite fibers at $\lambda = 3$ is responsible for the higher tensile strength. A similar effect of the drawing of fibers was observed with PP nanocomposite fibers containing 3 wt % (Sample E23/22) and 5 wt % (Sample E22; Table I). This explanation of the positive effect of the drawing of the fibers and the formation of exfoliated structures on the tensile strength of the fibers supports an observation that an increase of the filler content in the fibers (from 1 to 3 or 5 wt %) also increases the content of self-assembled structures. Thus, a considerable increase of the tensile strength of the fibers at the same drawing ratio [from 0.65 cN/dtex at 1 wt % filler (Sample E23) to 1.34 cN/dtex at 5 wt % filler (Sample E22), both prepared at $\lambda = 2$] can be expected.

Rheological study of the PP nanocomposite fibers

Influence of nanoparticles and compatibilizer on rheological properties of PP

Inorganic pigments (e.g., TiO_2) at concentrations of 1–3% have often resulted in a negligible influence on flow properties, such as viscosity. Similarly, we found little difference in flow behavior between natural PP and a dispersion of PP with nanoparticles of SOMASIF ME C16 and with 10% PP grafted with MA as compatibilizer.

PP alone in the melt behaves as a pseudoplastic liquid with a power law index of $n = 0.55$. Such

behavior indicates that the reactor has not degraded these relatively high viscosity polymers. Modified PP containing 10% compatibilizer and nanoparticles of the filler can be considered a polymer mixture with a higher cohesive energy density because of the presence of anhydride or carboxylic groups on the compatibilizer whose polar interactions lead to an increase of PP viscosity (Figure 15). An addition of nanoparticles of SOMASIF MC 16 to such a mixture causes a moderate increase in deviation from Newton flow (Power law index value is 0.51; Figure 16) for all filler concentrations. It is surprising that with increasing concentration of nanoparticles from 1 to 5 %, the melt viscosity of PP nanocomposites exhibits a moderate but unambiguous decrease.

Increasing of SOMASIF MC 16 concentration does not result in an increased tendency towards formation of labile agglomerates. The decrease of viscosity is possibly the result of "saturation" within a cluster of interacting anhydride groups of the compatibilizer with the surface of the solid filler particles. These regions do not disappear during the dispersion flow (they have nearly equal values of index, n). From this point of view, the interactions of the functional groups of the compatibilizer have a positive influence on flow properties of the nanocomposite melt (Figure 16).

CONCLUSIONS

Our objective in this paper was to determine the effect of one-dimensional orientation on the morphology and mechanical properties of PP nanocomposites in the form of fibers. Micrographs of PP composite fibers filled with SOMASIF ME C16 show that SOMASIF particles are oriented in the drawing direction of the fibers. Furthermore, a high degree of exfoliation of the SOMASIF particles in the fibers was observed following processing and spinning of PP composites and drawing of fibers. The level of exfoliation is directly proportional to the drawing ratio λ. At a drawing ratio of λ = 3, the distance between adjacent layers of the filler is ~10 nm. Almost the whole area of the micrograph of the parallel-cut fiber is filled in with SOMASIF sheets, which is the result of an exfoliation of the SOMASIF particles. Finally, increases in the SOMASIF filler content and drawing ratio of the fibers (from λ = 2 to λ = 3) have considerable effects on the tensile strength of the fibers.

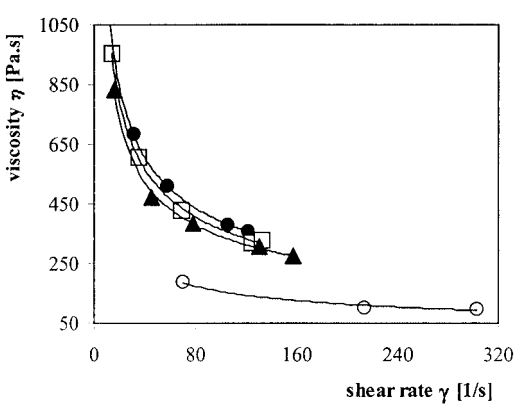

Figure 15 Rheological parameters (viscosity η and shear rate γ) of PP filled with SOMASIF. Key: (□) PP + 3 % SOMASIF; (▲) PP + 5 % SOMASIF.

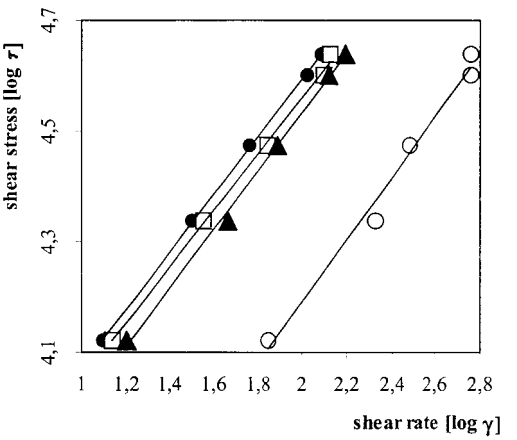

Figure 16 Rheological parameters (shear stress τ and shear rate γ) of PP filled with SOMASIF. Key: (○) PP; (●) PP + 1 % SOMASIF; (□) PP + 3 % SOMASIF; (▲) PP + 5 % SOMASIF.

This work was supported by Project VEGA1/6159/99, Slovak Republic.

References

1. Zilg, C.; Reichert, P.; Dietsche, F.; Engelhardt, T.; Mülhaupt, R. Kunststoffe 1998, 88, 1812.
2. Reichert, P.; Nitz, H.; Klinke, S.; Brandsch, R.; Thomann, R.; Mülhaupt, R. Macromol Mater Eng 2000, 275, 8.
3. Walter, P.; Mäder, D.; Reichert, P.; Mülhaupt, R. J Macromol Sci, Pure Appl Chem 1999, A36, 1613.
4. Ke, Y.; Lü, J.; Yi, X.; Zhao, J.; Qi, Z. J Appl Polym Sci 2000, 78, 805.
5. Zanetti, M.; Camino, G.; Thomann, R.; Mülhaupt, R. Polymer 2001, 42, 4501.
6. Zhang, M.Q.; Rong, M.Z.; Zeng, H.M.; Schmitt, S.; Wetzel, B.; Friedrich, K. J Appl Polym Sci 2001, 80, 2218.
7. Reichert, P.; Kressler, J.; Thomann, R.; Mülhaupt, R.; Stöppelmann, G. Acta Polym 1998, 49(2–3), 116.
8. Heinemann, J.; Reichert, P.; Thomann, R.; Mülhaupt, R. Macromol Rapid Commun 1999, 20(8), 423.
9. Zilg, C.; Thomann, R.; Mülhaupt, R.; Finter, J. Adv Mater 1999, 11(1), 49.
10. Dietsche, F.; Thomann, Y.; Thomann, R.; Mülhaupt, R. J Appl Polym Sci 2000, 75, 396.
11. Zilg, C.; Thomann, R.; Finter, J.; Mülhaupt, R. Macromol Mater Eng 2000, 280(7–8), 41.
12. Hoffmann, B.; Dietrich, C.; Thomann, R.; Friedrich, C.; Mülhaupt, R. Macromol Rapid Commun 2000, 21(1), 57.
13. Zilg, C.; Thomann, R.; Baumert, M.; Finter,J.; Mülhaupt, R. Macromol Rapid Commun 2000, 21(17), 1214.
14. Borsig, E.; Pavliková, S.; Marcinčin, A., unpublished data.